# Synthèse en français

## 0.1 Introduction

The modern scientific understanding of high energy physics rests on the success of theoretical and experimental approaches, achieved in the second half of the XX and beginning of XXI centuries. Current thesis is dedicated to the experimental study of the properties of a fundamental particle called the W boson and to the improvement of the experimental techniques used within the ATLAS experiment.

### 0.1.1 Le Modèle Standard des particules

The Standard Model of particle physics is a quantum field theory developed in the 1960s-1970s that describes structure and interaction of matter on the fundamental level. The theory postulates the existence of 12 elementary fermions and provides means to describe their interaction through 3 out of 4 known fundamental forces: electromagnetic, weak and strong. The mediators of these fundamental forces are also described as elementary particles (see Fig. 0.1). The predictions of the Standard Model depend on 18 input parameters that need to be measured experimentally.

The W and Z bosons are the carriers of weak interaction. The W boson was experimentally discovered in 1983 at CERN, the precision measurements of its mass and properties are ongoing ever since. With W boson is one of the cornerstones of the Standard Model, precision experimental measurements of its properties allow to test and improve theoretical predictions. This serves as a motivation for this thesis.

### 0.1.2 Le Grand Collisionneur de Hadrons (LHC) et lexpérience ATLAS

The Large Hadron Collider (LHC) is a particle accelerator built near the Swiss city of Geneva. Having the circumference of 27 km it is the biggest particle accelerator in the world. It is able to accelerate protons up to an energy of 6.5 TeV per particle and lead ions up to 2.76 TeV per nucleon. During the Run 2 the LHC delivered collimated beams to 4 interaction points at a rate of 40 million

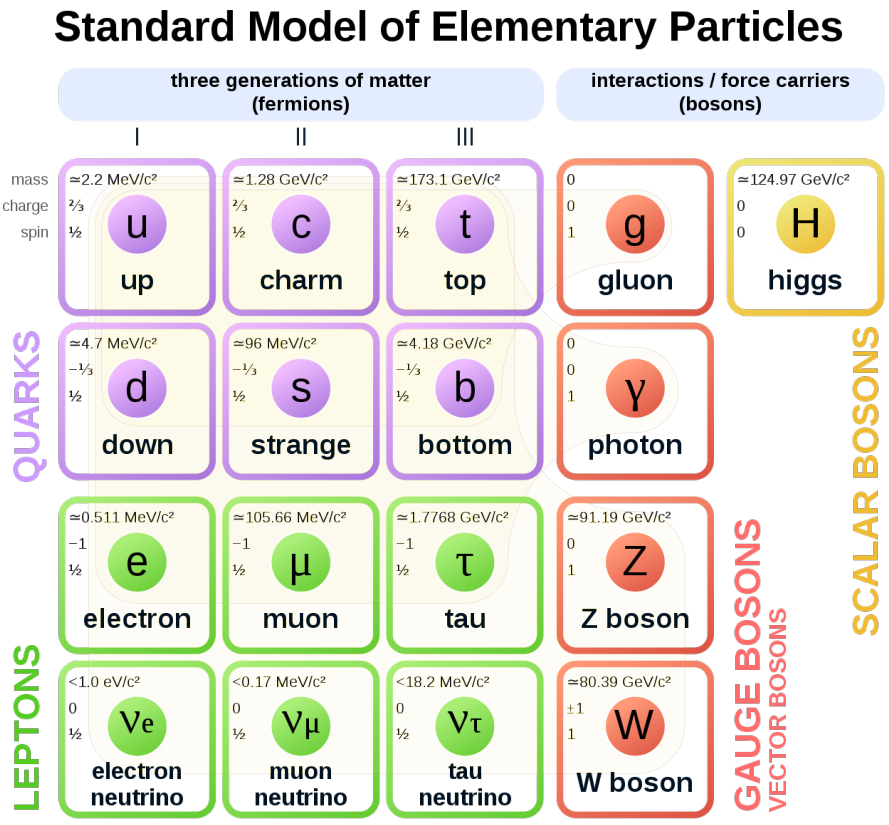


**Figure 0.1:** The list of particles that enters the Standard Model (SM).

bunch crossings per second. The four interaction points correspond to four experiments that are based on the LHC: ATLAS, CMS, LHCb and ALICE.

The ATLAS experiment is a multi-purpose cylindrical-shaped particle detector that is 44 m long and 25 m tall. It has an onion-like structure combining different types of detectors to allow the most efficient particle reconstruction (see Fig. 0.2). After the collision at the interaction point the outgoing particles penetrate the inner detector, that provides information about the direction, momentum and charge of the charged particles. Then the particles reach the calorimeter, that is used to reconstruct the energy and momentum of both neutral and charged particles. Finally, the particles that are able to penetrate the calorimeter reach the muon chambers which is the outermost detector system within the ATLAS calorimeter. The muon chambers are used to reconstruct the direction, momentum and charge of the muons.

### 0.1.3 Electromagnetic shower shapes correction

The electromagnetic calorimeter is designed to reconstruct the energy of electrons and photons that reach the calorimeter. The information from the electromagnetic calorimeter (EMC) is also used

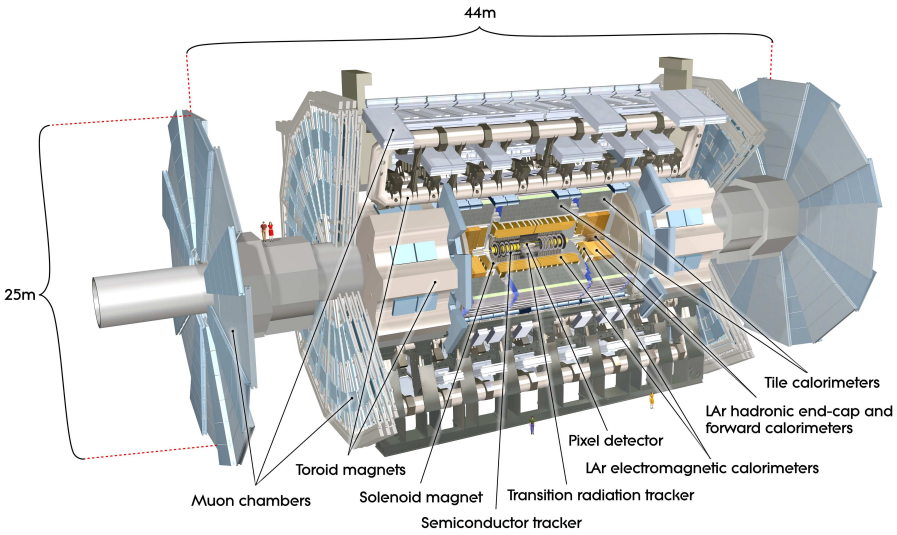


**Figure 0.2:** ATLAS detector general layout.

for particle identification and background rejection.

The EMC consists of three layers and a presampler (see Fig. 0.3). The second layer is the thickest one, it absorbs most of the energy of electrons and photons. The second layer has a fine granularity in both $\eta$ and $\phi$ dimensions, that provides the information on the transverse development of the electromagnetic shower. This information is used to introduce a number of observables that are called the shower shapes and then used as an input for a likelihood-based MVA algorithm which makes a decision on particle identification. There are three shower shapes that reflect the shower development in the third calorimeter layer:

- Lateral shower width $W_{\eta 2} = \sqrt{\sum(E_i \eta_i^2) - (\sum(E_i \eta_i)/\sum(E_i))^2}$ calculated within a window of 3x5 cells.
- $R_\phi$ - ratio of the energy in 3x3 cells over the energy in 3x7 cells centered around the hottest cell.
- $R_\eta$ - ratio of the energy in 3x7 cells over the energy in 7x7 cells centered around the hottest cell.

For some reasons that are not particularly clear the Monte-Carlo modelling of the shower shapes is flawed and there is a substantial discrepancy with the data (see Fig. 0.4). These discrepancies have to be corrected with the scale factors, which in turn introduce the $p_T$-associated uncertainties. This thesis presents a data-driven method to correct for these discrepancies by redistributing the energy between the cells of the calorimeter cluster.

The corrected shower shapes in Monte-Carlo demonstrate good agreement with the data and result in significantly better agreement in identification efficiencies (see Fig. 0.5). The correction effect is the most prominent in the end-cap region where it reaches 3%. The proposed method has been integrated into the official framework of the ATLAS experiment and will be used as a baseline for Run 3 analyses.

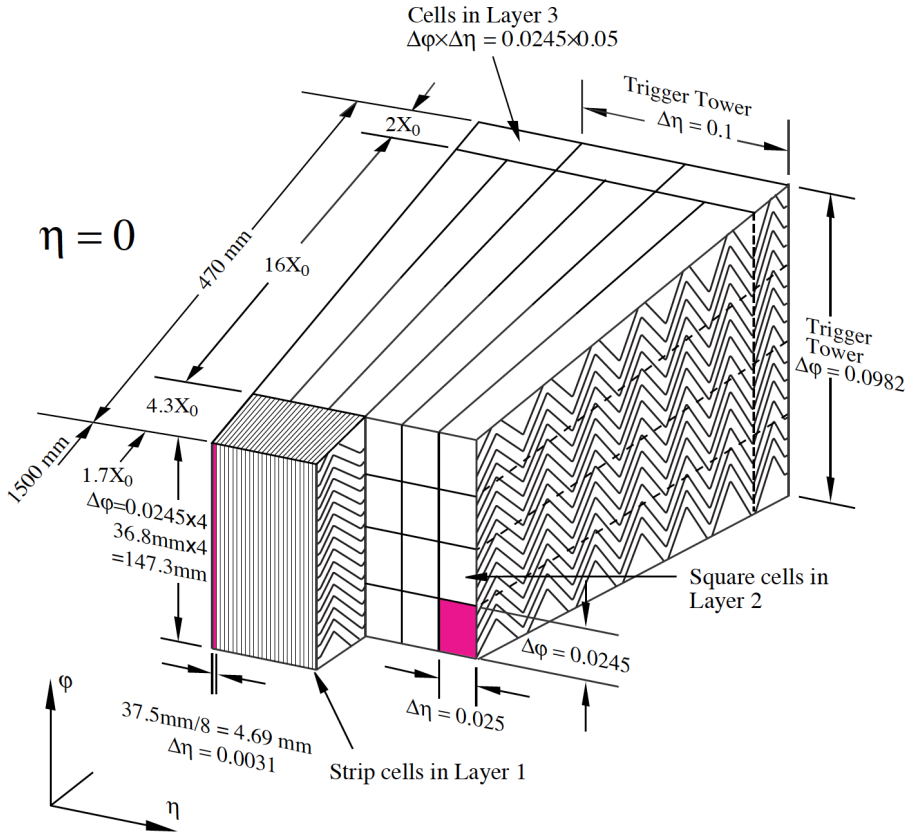


**Figure 0.3:** ATLAS EM calorimeter layers.

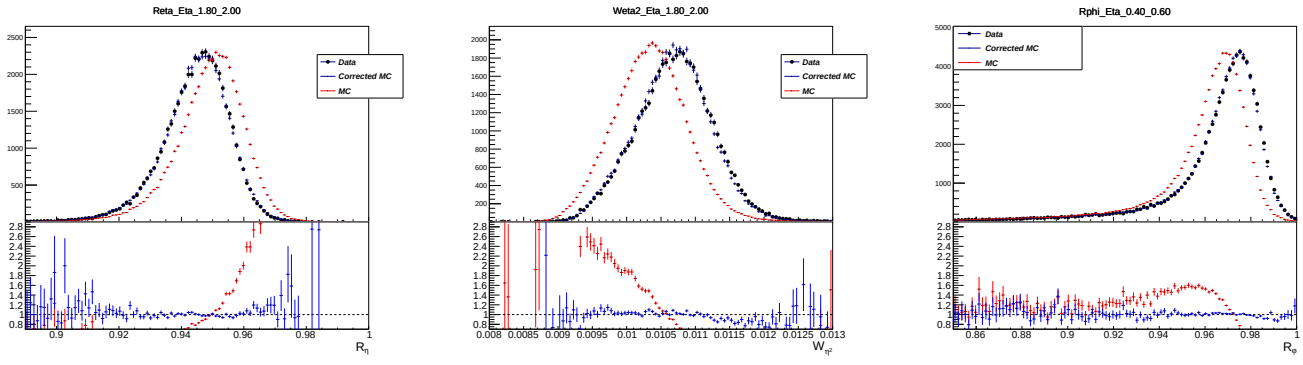


**Figure 0.4:** **Left**: $R_\eta$ in $|\eta| = (1.8, 2.0)$. **Central**: $W_{\eta^2}$ in $|\eta| = (1.8, 2.0)$. **Right**: $R_\phi$ in $|\eta| = (0.4, 0.6)$.

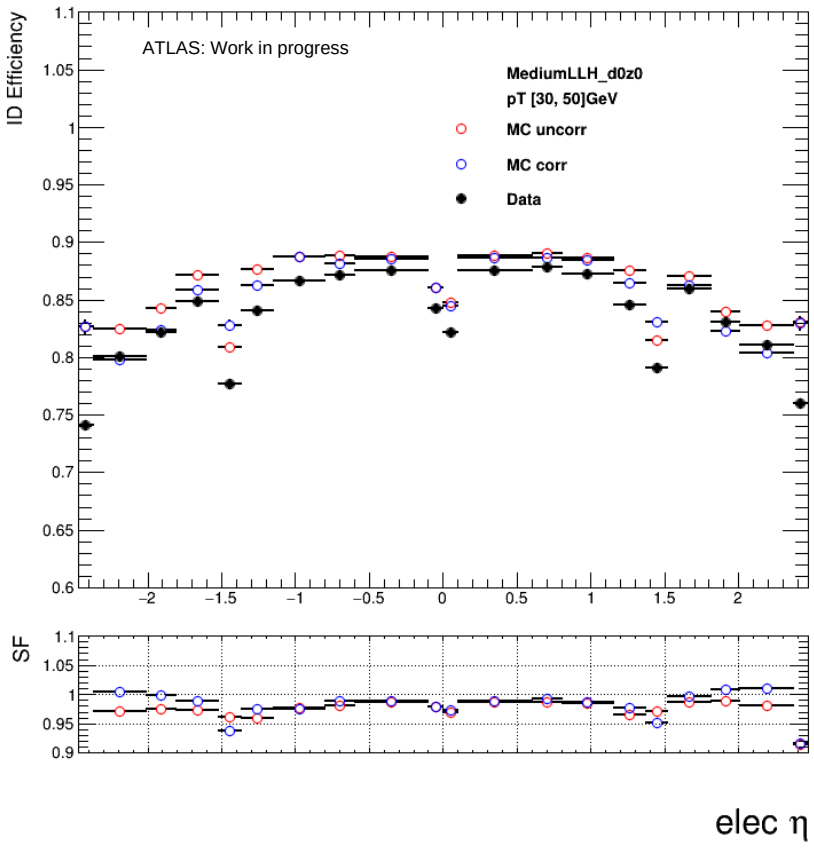


**Figure 0.5:** Electron identification efficiency as a function of the electron pseudo-rapidity.

### 0.1.4 W boson transverse momentum spectrum

The measurement of the W boson transverse momentum spectrum is a challenging yet important task. At the leading order (Fig. 0.6a) the W boson $p_T$ is mainly caused by the intrinsic parton movement and does not exceed 1 GeV. The observed W boson transverse momentum distribution that reaches hundreds of GeV is due to the initial state radiation, which is a next-to-leading order process (see Fig. 0.6b). This allows to test the credibility of the Standard Model predictions, comparing the Monte-Carlo to the data.

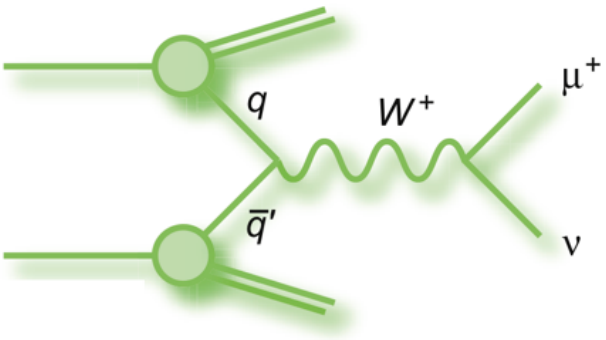


(a) Leading order Feynman diagram of W boson production.

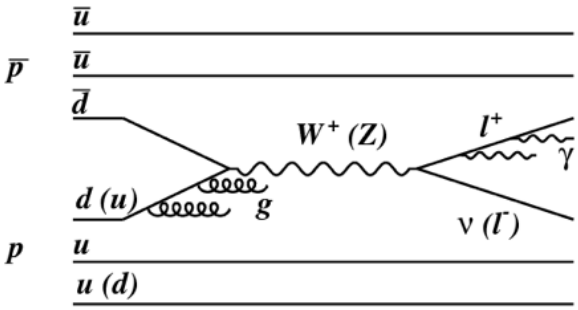


(b) W boson production in NLO.

The second motivation comes from the fact that the W transverse momentum spectrum distribution is necessary for the precise measurement of the W boson mass. Being one of the input parameters of the Standard Model, the precision of this measurement has implications on all the predictions of the theory. The W $p_T$ theoretical modelling was the second-dominant uncertainty in the previous ATLAS measurement of the W boson mass.

At the same time the measurement of the transverse momentum is rather complicated. Because of the escaping neutrino it is impossible to reconstruct the W boson $p_T$ directly from its decay products. Instead of that the W $p_T$ distribution is reconstructed using an observable called the hadronic recoil. The hadronic recoil is supposed to reflect the transverse momentum of the initial state radiation and be equal in magnitude and antiparallel to the W boson $p_T$ (see Fig. 0.7a). It is defined as a vector sum of all the particle flow objects (PFOs) in the event, excluding the vector boson decay products. The resolution of the hadronic recoil directly depends on the pile-up (Fig. 0.7b), which motivated to use the low pile-up dataset, collected by the ATLAS experiment in 2017 and 2018.

Although the hadronic recoil is very correlated with the real W boson $p_T$, the shape of the distribution can be very different due to the detector effects. In order to restore the underlying distribution a procedure called unfolding is used. After unfolding the hadronic recoil it becomes possible to compare the obtained distribution with MC predictions.

It appears that the measured spectrum demonstrates fair agreement with the MC models at 5 TeV, while at 13 TeV none of the MC generators provides a compatible prediction.

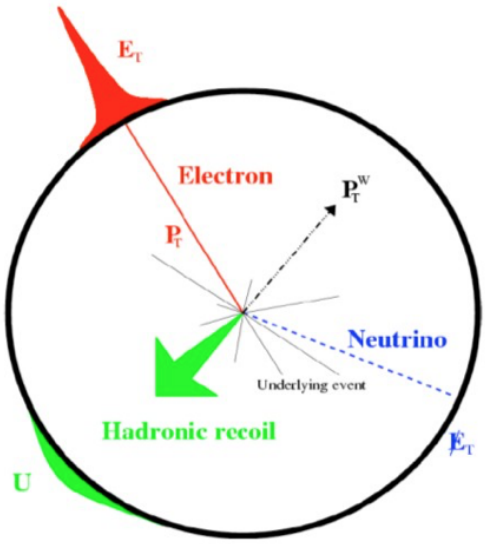


(a) The hadronic recoil.

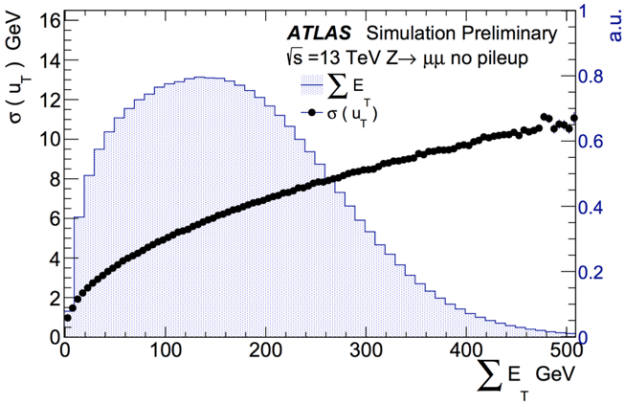


(b) Hadronic recoil dependence on pile-up.

**Figure 0.7:** The hadronic recoil plots.

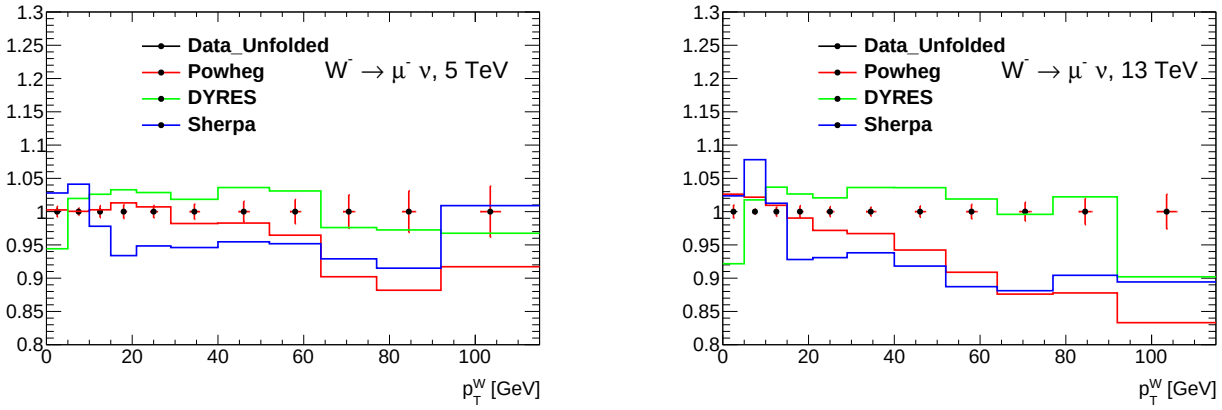


**Figure 0.8:** Unfolded spectrum compared to MC models for the $W^- \to \mu^- \nu$ at 5 TeV (left) and 13 TeV (right).

### 0.1.5 Hadronic recoil reconstruction using deep neural networks

The resolution of the hadronic recoil measurement is crucial for the determination of W $p_T$ spectrum distribution. Modern methods of data analysis provide means to improve the resolution on event-by-event basis. In order to improve the resolution a deep neural network has been used with the following parameters:

- Training sample: 12 734 109 events, validation sample: 3 034 130 events.
- Framework: Keras/Tensorflow.
- Loss function: mean square error.
- Optimizer: Adam, step: 0,001.
- Batch size: 3900 events.
- Three hidden dense layers with 256 nodes each.
- batch normalization layer after each hidden layer.

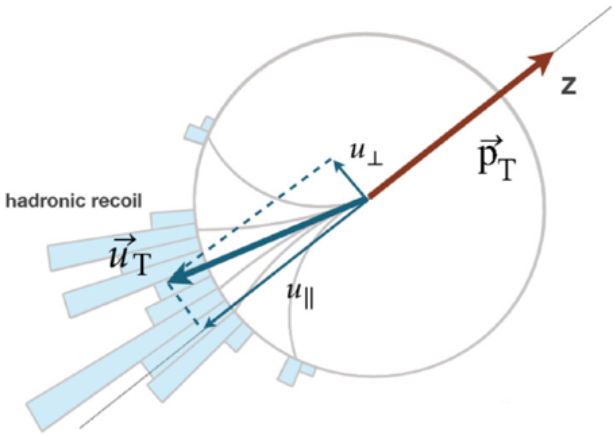


(a) Hadronic recoil decomposition.

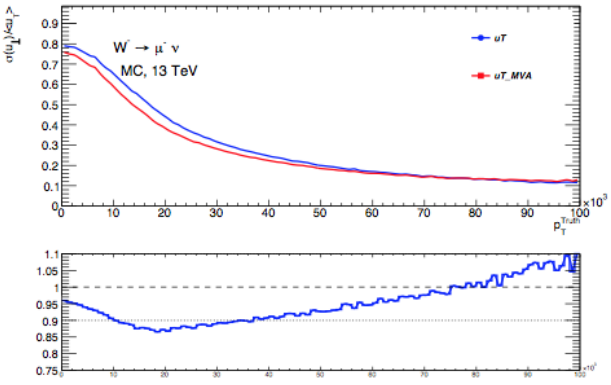


(b) HR resolution improvement with DNN.

This configuration has been tested to be the most effective under given conditions. The batch normalization has improved the stability of the fit and reduced training time roughly by a factor of five. The following list of input features was used:

- The hadronic recoil vector $\vec{u_T}$.
- $u_T^{\vec{charged}}$ - vector sum of charged PFOs $\vec{p_T}$.
- $u_T^{\vec{neutral}}$ - vector sum of neutral PFOs $\vec{p_T}$.

- $\Sigma E_T$, $\Sigma E_T^{charged}$, $\Sigma E_T^{neutral}$ - scalar sums of transverse energies.
- Leading and subleading jets $p_T$s.
- Number of primary vertices per event.
- Number of charged and neutral PFOs in the event.
- Transverse momenta of five leading neutral and charged PFOs.

It sums up to a total of 38 input features for the regression of two components of the W boson $\vec{p_T^{truth}}$.

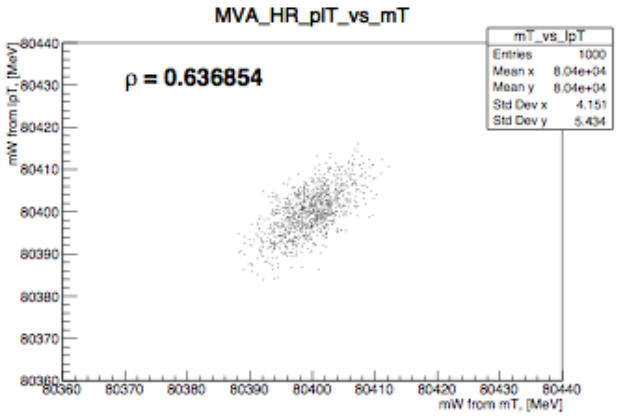


(a) Bootstrap test for the nominal hadronic recoil.

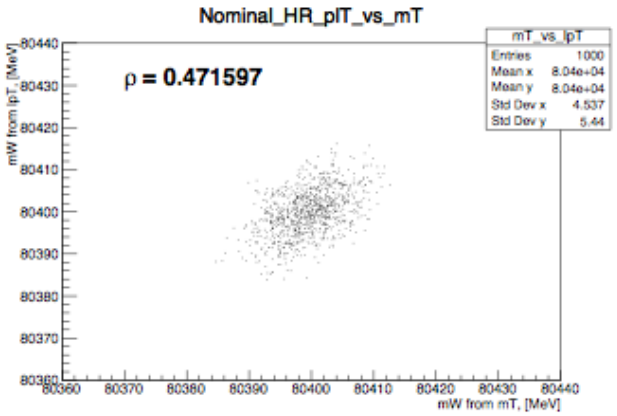


(b) Bootstrap test for the nominal NN-reconstructed hadronic recoil.

Due to the detector effects the hadronic recoil vector is different from the true W boson $p_T$ in magnitude and is not antiparallel to it (see Fig. **??**). The resolution of the hadronic recoil can be represented as the spread of the perpendicular component of the hadronic recoil $\sigma(u_\perp)$. The plot at Fig. 0.9b demonstrates about 10% of improvement coming from using the deep neural network for hadronic recoil reconstruction.

Improved hadronic recoil resolution also results in a better sensitivity of the observables to the W boson mass. This was tested using 1000 bootstrap toys and has shown a smaller spread in the transverse mass when using the neural network (See Figs. 0.10a and 0.10b ).

### 0.1.6 Conclusions

This thesis has presented three main contributions that are related to the measurement of the W boson properties and to overall performance of the ATLAS detector.

Correction of the shower shapes in the electromagnetic calorimeter has allowed to correct the identification efficiency in the MC, gaining 1-3% in the end-cap region. The developed algorithm has been adopted as a baseline for the upcoming Run 3 analyses within the ATLAS experiment.

The measurement of the W boson transverse momentum distribution has allowed to perform comparison with the existing MC models. The comparison has revealed a fair agreement at 5 TeV, but a significant discrepancy at 13 TeV. The achieved precision would allow to significantly reduce theoretical modelling uncertainty for the W boson mass measurement.

The usage of deep learning algorithms has allowed to improve the reconstruction of the hadronic recoil, allowing about 10% improvement in the resolution in the most important region of low transverse momentum. It has also resulted in the increased sensitivity of the observables to the W boson mass, which was tested using the bootstrap method.